Surface properties of heterogeneous polycyclic aromatic hydrocarbon clusters - Supplemental Material

Kimberly Bowal[a], Laura Pascazio[a], Hongyu Wang[b], Dongping Chen[b,*],
Markus Kraft[a,c,**]

[a]*Department of Chemical Engineering and Biotechnology, University of Cambridge, Cambridge CB3 0AS, United Kingdom*
[b]*Department of Mechatronical Engineering, Beijing Institute of Technology, Beijing 100081, China*
[c]*School of Chemical and Biomedical Engineering, Nanyang Technological University, 637459, Singapore*

1. Position potential

Following the methodology reported in Ref. [1], a position potential aligned with a spherical volume is applied within replica exchange molecular dynamics simulations. This is a flat-bottomed potential, shown in Equation 1, that only applies a force on a molecule once it leaves the cluster, allowing all molecules within the cluster to move unaffected by the potential. The force applied acts towards the centre of the spherical volume and is independent of PAH size.

$$E_{\text{pos}}(r_i) = \frac{1}{2}k_{\text{pos}}\left(|r_i - R| - r_{\text{pos}}\right)^2 \text{H}\left(|r_i - R| - r_{\text{pos}}\right) \tag{1}$$

where E_{pos} is the position potential energy for a single atom i in kJ mol^{-1}, r_i is the coordinate position of atom i, R is the geometric centre of the cluster,

*Corresponding author
**Principal corresponding author
Email addresses: `dc516@bit.edu.cn` (Dongping Chen), `mk306@cam.ac.uk` (Markus Kraft)

r_{pos} is the position potential radius, $k_{\mathrm{pos}} = 1000$ kJ mol^{-1}nm^{-2} is the force constant, and H is the Heavyside step function. The position potential is necessary for minimum energy configurations to be attained since it allows the replicas to efficiently sample configurational space. Importantly, this applied potential is negligible at temperatures below the cluster melting point and low energy configurations are not affected by the position potential.

2. Replica exchange molecular dynamics temperature distribution

Replica temperatures were selected using an exponential temperature distribution

$$T_j = T_0 \exp(mj) \tag{2}$$

where T_j refers to the temperature (in K) at replica j, T_0 is the temperature (K) at replica 0, and m is a parameter which achieves the desired temperature range.

The temperature ranges are selected to encompass both solid- and liquid-like configurations. In these heterogeneous clusters the temperature ranges differ with the molecular composition of the cluster, since constituent molecule sizes determine the temperature at which a cluster is liquid- or solid-like. The smallest molecule present determines the lower temperature bound, with pyrene at 200 K and coronene at 400 K. Similarly the largest molecule present determines the upper temperature bound, with ovalene at ≥ 800 K and circumcoronene at ≥ 1600 K.

The j and m parameters, shown in Table S1, are selected for each cluster system to allow satisfactory exchange between replicas (discussed further below) using these temperature ranges.

2

Table S1: Temperature range parameters for heterogeneous particles considered in this work. Systems labelled by an asterisk were taken from Ref. [1].

Cluster type	Number of molecules	m	j
Binary 50% OVA, 50% PYR	4	0.107	$0 - 13$
	32*	0.035	$0 - 39$
	100*	0.024	$0 - 59$
Binary 50% CIR, 50% COR	4	0.093	$0 - 15$
	32*	0.035	$0 - 39$
	100*	0.024	$0 - 59$
Quaternary (uniform) 25% CIR, 25% OVA, 25% COR, 25% PYR	4	0.091	$0 - 23$
	32	0.036	$0 - 59$
	100*	0.028	$0 - 74$
Quaternary (nonuniform) 40% CIR, 30% OVA, 20% COR, 10% PYR	10	0.054	$0 - 39$
	24	0.036	$0 - 59$
	100	0.024	$0 - 87$

The effectiveness of an REMD simulation relies on the proper exchange of states between replicas so that the low temperature states are able to sample the high temperature configurations and vice versa. Replica exchange acceptance is a good indication of the movement between replicas and it is found empirically and theoretically that an exchange acceptance of approximately 0.2 provided the best accuracy for a given computational time [2, 3]. Exchange acceptances for simulations conducted in this work are approximately $0.2 - 0.4$, which indicates a good balance between equilibration within each replica and exchange between replicas.

3. Surface densities of edge carbon atoms and free-edge sites

The density of edge carbon atoms on the particle surface, χ_{EC}, is not affected by temperature or particle size, and can therefore be described by the molecular composition alone. As seen in Figure S1(a), the contribution of edge carbon atoms to the surface decreases as the constituent molecule size increases, with homogeneous circumcoronene, ovalene, coronene, and pyrene particles presenting values of approximately 3.5×10^{18}, 4.6×10^{18}, 5.2×10^{18}, and 6.7×10^{18}, respectively. A weighted average of these values provides a good prediction of heterogeneous particles examined in this work (for example, a CIRCOR particle is an average of CIR and COR values), leading to the simple linear trend shown in Figure S1(b). This relationship allows us to estimate the density of edge carbons on the particle surface from an average molecule length value, such as that determined by fringe analysis of high resolution transmission electron microscopy images. As an example, Ref. [4] gives an average fringe length value of 0.80 nm for young soot produced in a benzene flame. We can estimate that these particles have a surface density of 6.1×10^{18} atoms of edge carbon per m^2.

As seen in Figure S2, the surface density of free-edge sites, χ_{FE}, shows similar behaviour, although there is a slight decrease in χ_{FE} with increasing temperature due to the increasing contribution of large molecules to the surface. The linear trend provided relates the surface density of FE sites with the average molecule length.
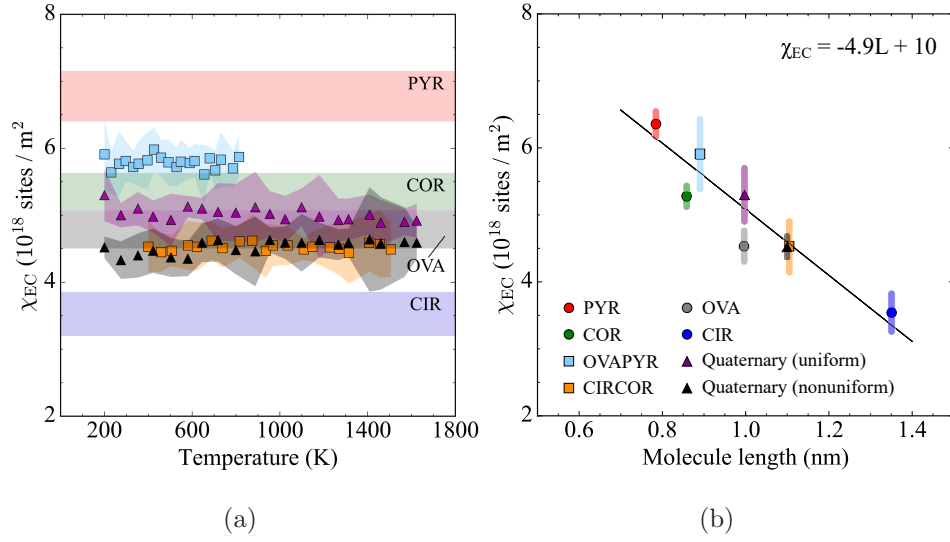
4

Figure S1: Edge carbon atom density on the particle surface, χ_{EC}, as a function of the temperature (a) and average molecule length, L (b) for particles with a diameter of 3 nm.
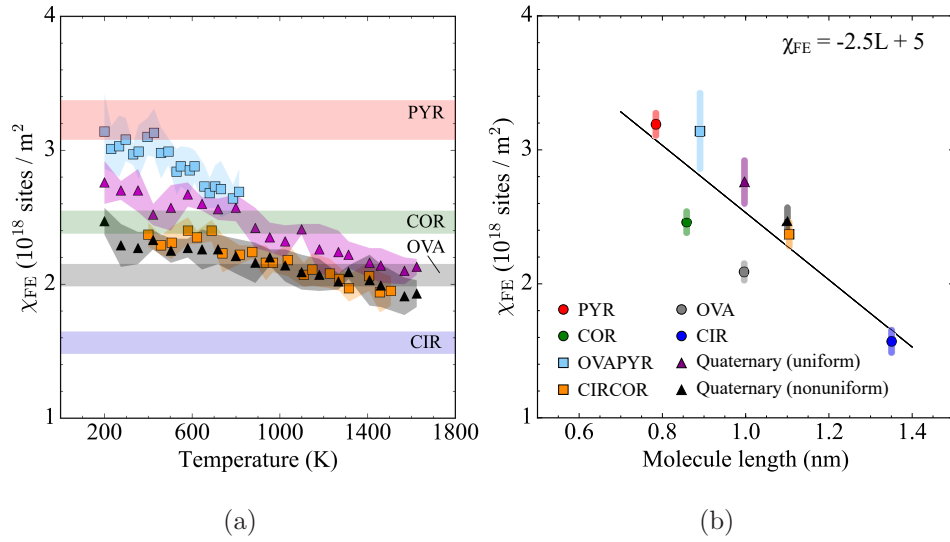

Figure S2: Free-edge site density on the particle surface, χ_{FE}, as a function of the temperature (a) and average molecule length, L (b) for particles with a diameter of 3 nm.

4. Parameter α for 5 nm particles

The parameter α is strongly dependent on temperature, with particle diameter playing a weaker role. Figure S3 shows values of the parameter α across a wide range of temperatures for homogeneous and heterogeneous particles approximately 5 nm in diameter. As in the 3 nm case reported earlier, the heterogeneous particle α parameter values reflect an average of the homogeneous constituents and simple linear relationship can be used to approximate α of heterogeneous particles as a function of temperature.
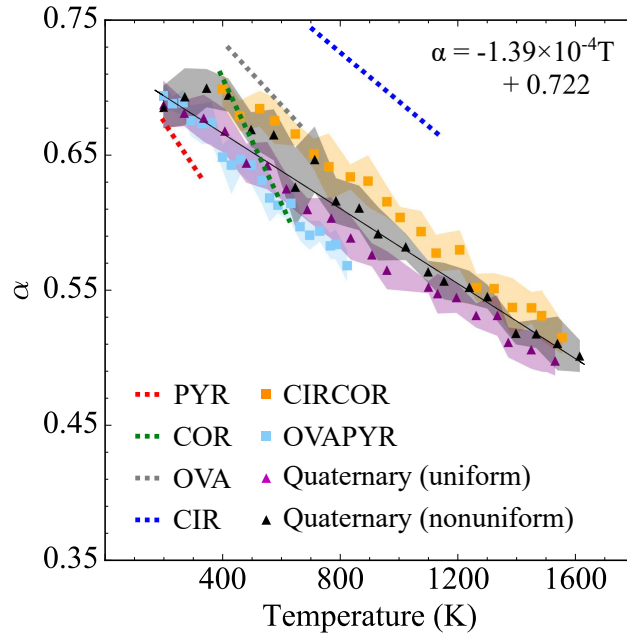

Figure S3: Parameter α for particles with a diameter of approximately 5 nm as a function of temperature. Shaded areas show the standard deviation of heterogeneous particle values. Homogeneous particle values, taken from Ref. [5], are shown as dashed lines. A single trend line is shown for all of the heterogeneous cases.

5. Atom/site percent versus particle diameter

A larger version of Figure 2 is included here as Figure S4.
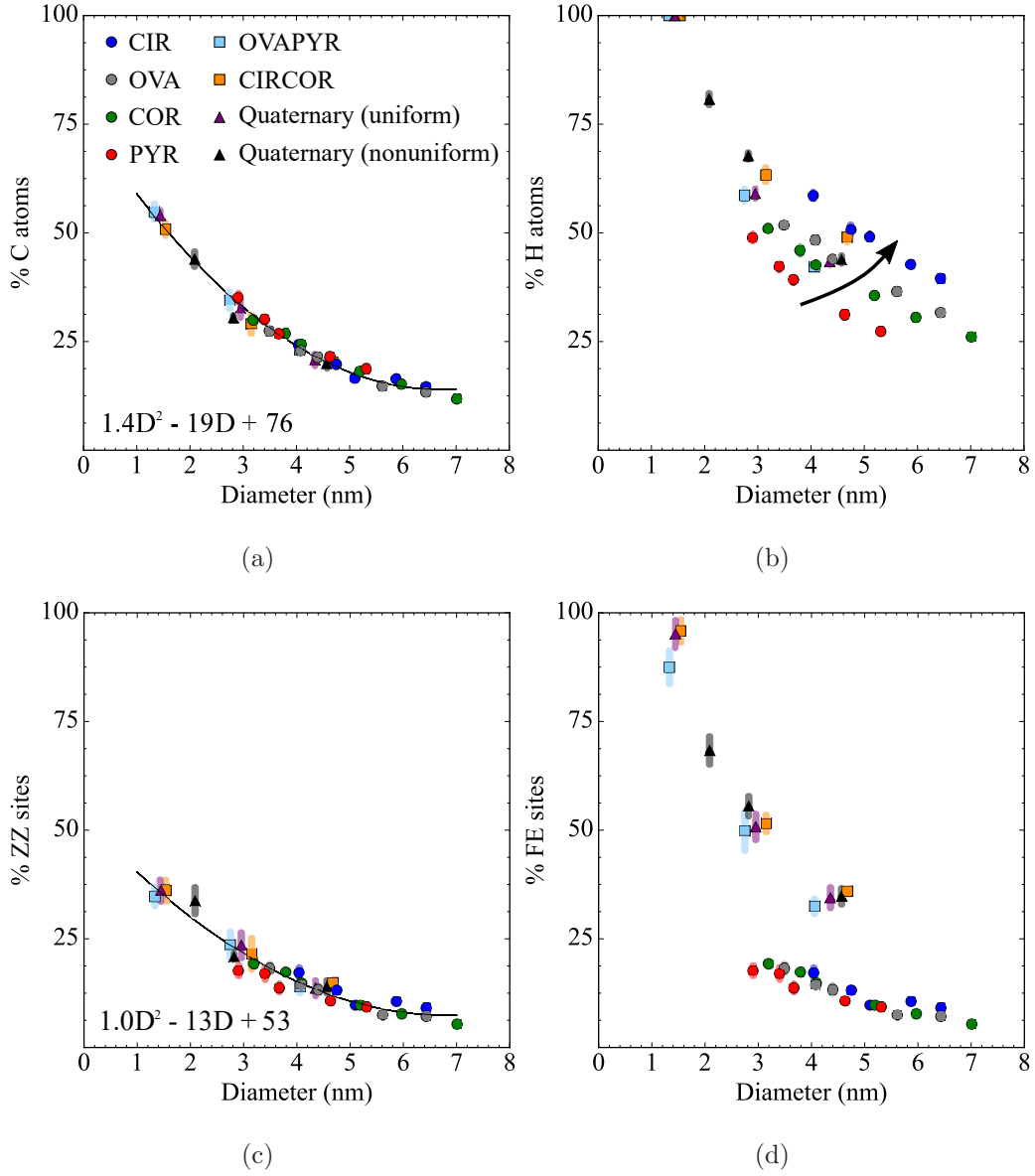
Figure S4: Percentage of (a) carbon atoms, (b) hydrogen atoms, (c) ZZ sites, and (d) FE sites present on the particle surface for homogeneous and heterogeneous particles at solid-like configurations. Shaded areas indicate the standard deviation. The arrow in (b) indicates the effect of increasing molecule size. Homogeneous particle values are taken from Ref. [5].

References

[1] K. Bowal, J. W. Martin, M. Kraft, Partitioning of polycyclic aromatic hydrocarbons in heterogeneous clusters, *Carbon* 143 (2019) 247–256.

[2] N. Rathore, M. Chopra, J. J. De Pablo, Optimal allocation of replicas in parallel tempering simulations, *J. Chem. Phys.* 122 (2005) 24111–174903.

[3] A. Kone, D. A. Kofke, Selection of temperature intervals for parallel-tempering simulations, *J. Chem. Phys.* 122 (2005) 206101.

[4] M. Alfè, B. Apicella, R. Barbella, J.-N. Rouzaud, A. Tregrossi, A. Ciajolo, Structure–property relationship in nanostructures of young and mature soot in premixed flames, *Proc. Combust. Inst.* 32 (2009) 697–704.

[5] D. Chen, J. Akroyd, S. Mosbach, M. Kraft, Surface reactivity of polycyclic aromatic hydrocarbon clusters, *Proc. Combust. Inst.* 35 (2015) 1811–1818.